Electrochimica Acta 56 (2011) 4243–4247

Contents lists available at ScienceDirect

Electrochimica Acta

journal homepage: www.elsevier.com/locate/electacta

High lithium ion conducting Li_2S–GeS_2–P_2S_5 glass–ceramic solid electrolyte with sulfur additive for all solid-state lithium secondary batteries

James E. Trevey[a], Yoon Seok Jung[b], Se-Hee Lee[a,*]

[a] Department of Mechanical Engineering, University of Colorado at Boulder, Boulder, CO 80309-0427, USA
[b] Present address: National Renewable Energy Laboratory, Golden, CO 80401, USA

ARTICLE INFO

Article history:
Received 15 December 2010
Received in revised form 21 January 2011
Accepted 22 January 2011
Available online 28 January 2011

Keywords:
Lithium battery
Solid-state battery
Solid-state electrolyte
Sulfide
Lithium cobalt oxide

ABSTRACT

Glass–ceramic Li_2S–GeS_2–P_2S_5 electrolytes were prepared by a single step ball milling (SSBM) process. Various compositions of $Li_{4-x}Ge_{1-x}P_xS_4$ from $x = 0.70$ to $x = 1.00$ were systematically investigated. Structural analysis by X-ray diffraction (XRD) showed gradual increase of the lattice constant followed by significant phase change with increasing GeS_2. All-solid-state $LiCoO_2$/Li cells were tested by constant-current constant-voltage (CCCV) charge–discharge cycling at a current density of 50 $\mu A\,cm^{-2}$ between 2.5 and 4.3 V (*vs.* Li/Li^+). In spite of the high conductivity of the solid-state electrolyte (SSE), $LiCoO_2$/Li cells showed a large irreversible reaction especially during the first charging cycle. Limitation of instability of Li_2S–GeS_2–P_2S_5 in contact with Li was solved by using double layer electrolyte configuration: $Li/(Li_2S\text{-}P_2S_5/Li_2S\text{–}GeS_2\text{–}P_2S_5)/LiCoO_2$. $LiCoO_2$ with SSEs heat-treated with elemental sulfur at elevated temperature exhibited a discharge capacity of 129 mA h g^{-1} at the second cycle and considerably improved cycling stability.

1. Introduction

Lithium secondary batteries prevail as one of the most widely accepted power sources for portable electronics and mobile devices because of their superior performance over other rechargeable batteries [1]. While they have great potential for high energy density and long cycle life, as well as being lightweight, most of these batteries uses liquid electrolytes that are flammable and hazardous [2,3]. Replacing the liquid electrolytes with solid state electrolytes (SSEs) would effectively eliminate the safety concern associated with the liquid electrolyte [4,5]. However, low ionic conductivity and interfacial instability stand in the way of the commercialization of all-solid-state rechargeable lithium-ion batteries [6,7].

Ball-milling has recently emerged as a more enticing method for SSE development over the melt quenching method [8]. The ball-milling process is relatively low cost and produces ultra-fine powders good for achieving high interfacial contact area between active materials and SSE powders [9]. Ball-milled SSE powders are often heat treated to achieve a crystalline structure capable of even higher conductivities than those reached by amorphous powder [10–12]. Furthermore, it has been shown that addition of a network former such as $GeSe_2$ to the Li_2S–P_2S_5 system results in even higher conductivity [9].

We have prepared sulfide-based lithium ion conducting SSE by the single-step ball-milling (SSBM) procedure [13], which combines ball-milling and heat treatment (HT) into one step. The Li_2S–GeS_2–P_2S_5 glass–ceramic electrolytes produced by SSBM exhibit high conductivities over 1×10^{-3} S cm^{-1} at ambient temperature. The all-solid-state cells with these SSE were confirmed to work as lithium secondary batteries. We also report on the inclusion of elemental sulfur into the Li_2S–GeS_2–P_2S_5 system which showed improved cycling stability and first cycle coulombic efficiency of $Li/LiCoO_2$ all-solid-state cells. While it is well known that sulfur is highly insulating and its incorporation into electrolytes typically shows decreased ionic conductivity, it has a highly polarizable character that has potential to improve stabilization of electrolyte in contact with the electrode. Elemental sulfur was chosen for enhancing the cycling stability of the electrolyte for its highly polarizable character, as high polarizability of anions is well known to aid the formation of strong covalent bonds between the anions of the framework, effectively orienting charge density away from the interstitial ions and improving ion conduction [14].

2. Experimental

SSEs were prepared by SSBM of Li_2S–GeS_2–P_2S_5 for 20 h [9,13]. Reagent-grade powders of Li_2S (Aldrich, 99.999%), P_2S_5 (Aldrich, 99%), and GeS_2 (City Chemical, 99.99%) were used as starting materials. Appropriate concentrations of materials were combined into a zirconia vial (Spex) at a net weight of 1 g with two zirconia

* Corresponding author.
E-mail address: sehee.lee@colorado.edu (S.-H. Lee).

0013-4686/$ – see front matter © 2011 Elsevier Ltd. All rights reserved.
doi:10.1016/j.electacta.2011.01.086

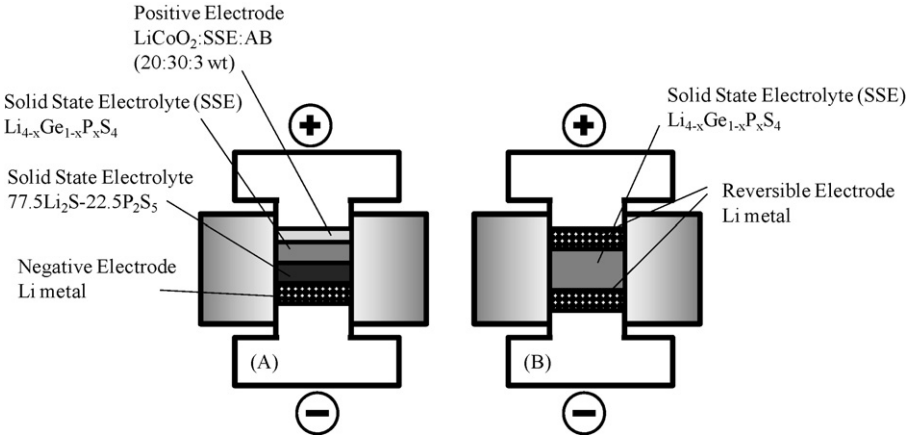

Fig. 1. Schematic diagram of Ti test die for (A) the all-solid-state battery and (B) measuring conductivity of SE.

balls (1 × 12 mm, 1 × 15 mm in diameter) for grinding. High energy ball milling (Spex8000) took place for 20 continuous hours in an Ar-filled dry box. Heat treatment of SSBM SSE powders was performed by first mixing sulfur and SSE powders in mortar and pestle and pelletizing the powders at 8 metric tons in a stainless steel die (ϕ = 1.3 cm) with 400 mg of starting material. Extracted pellets were placed in a sealed glass container and heated on a hot plate to 240 °C at approximately 10 °C min^{-1} for 16 h. With the starting time corresponding to the point when the hot plate reached the desired temperature, finished pellets were removed from the hot plate and placed on a cooling rack. The heat-treated pellets were then ground in a mortar with pestle and used for solid battery production with no further modifications. All pelletization and heat treatment processes were performed in a dry Ar filled glove box.

Composite electrodes were prepared by mixing $LiCoO_2$ powder (Sigma–Aldrich) as the active material, SSE Li_2S–GeS_2–P_2S_5 powder for fast lithium ion conduction, and acetylene black (Alfa-Aesar, 50% compressed) for electron conduction at a weight ratio of 20:30:3, respectively. Bilayer electrolyte pellets are formed by hand pressing 100 mg of Li_2S–GeS_2–P_2S_5 SE on top of a 100 mg hand pressed layer of $77.5Li_2S$–$22.5P_2S_5$ (mol%) SE prepared by the SSBM procedure. A 10 mg layer of the composite cathode material is then carefully spread on the top of the Li_2S–GeS_2–P_2S_5 electrolyte layer and the cell pelletized by cold pressing (5 metric tons) for 5 min. Li foil (Alfa-Aesar, 0.75 mm thick) is then attached to the $77.5Li_2S$–$22.5P_2S_5$ (mol%) SSE face at 2 metric tons. All pressing and testing operations are carried out in a polyaryletheretherketone (PEEK) mold (ϕ = 1.3 cm) with Ti metal rods as current collectors for both working and counter electrodes. All processes were carried out in an Ar-filled dry box. Galvanostatic charge–discharge cycling took place at first cycle cut off voltages of 4.1 and 2.5 V while the remaining cycles were run from 2.5 to 4.3 V at a current of 50 μA cm^{-2} at room temperature using Arbin BT2000.

SSE samples were characterized by XRD measurement with Cu Kα radiation. Samples were sealed in an airtight aluminum container with beryllium windows and mounted on the X-ray diffractometer (PANalytical, PW3830). Ionic conductivities were measured by AC impedance spectroscopy (Solartron 1280C). Weighed materials are cold pressed at 5 metric tons, before lithium metal plates are pressed to both sides of the pellet at 1 metric ton to serve as electrodes. The impedance of selected cells was measured from 20 MHz to 100 mHz at room temperature and the conductivity was determined using complex impedance analysis. Schematic diagrams for the Li/SSE/$LiCoO_2$ cells and AC impedance cells can be seen in Fig. 1(A) and (B), respectively.

3. Results and discussion

A schematic diagram for ternary component Li_2S–GeS_2–P_2S_5 is shown in Fig. 2. As x in $Li_{4-x}Ge_{1-x}P_xS_4$ increases, GeS_2 decreases and P_2S_5 increases with relatively small changes of Li_2S, and finally x = 1.00 corresponds with $75Li_2S$–$25P_2S_5$ (mol%).

Fig. 3(A) shows the recorded conductivities of the $Li_{4-x}Ge_{1-x}P_xS_5$ (Li_2S–GeS_2–P_2S_5) electrolyte in the range of $0.70 < x < 1.00$. We show that the SSBM procedure is superior to conventional ball-milling by approximately a factor of two for achieving extremely high conductivities when compared to the results obtained by Yamamoto et al. [15]. High conductivities were observed for the entire range of compositions with values ranging from 5.0×10^{-4} S cm^{-1} at the lowest and 1.2×10^{-3} S cm^{-1} at the highest but with most values recording around 1×10^{-3} S cm^{-1} as shown in Table 1. The highest recorded value for conductivity corresponds to the composition of x = 0.95, which corresponds to the molar composition of constituent compounds as $74.4Li_2S$–$2.4GeS_2$–$23.2P_2S_5$. This composition is that of the highest recorded conductivity for the Li_2S–GeS_2–P_2S_5 system studied by Yamamoto et al. as well. We attribute the high ionic conductivities of this system to the mixed-anion effect which

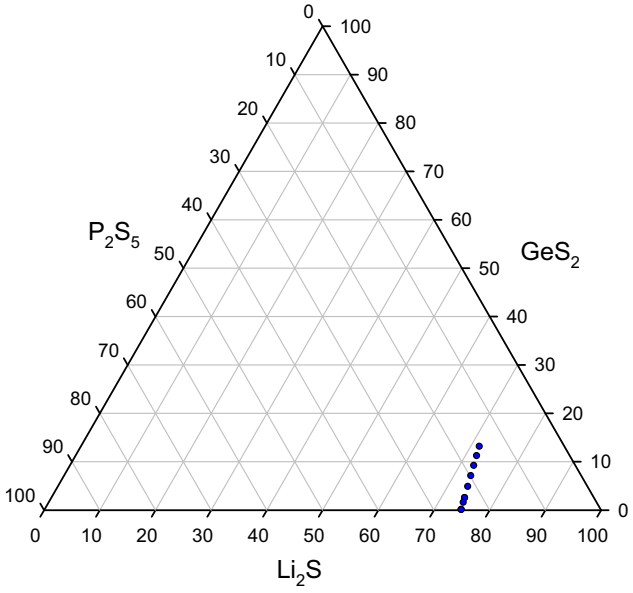

Fig. 2. Diagram for ternary components of Li2S–GeS_2–P2S5 which is also expressed as $Li_{4-x}Ge_{1-x}P_xS_4$.

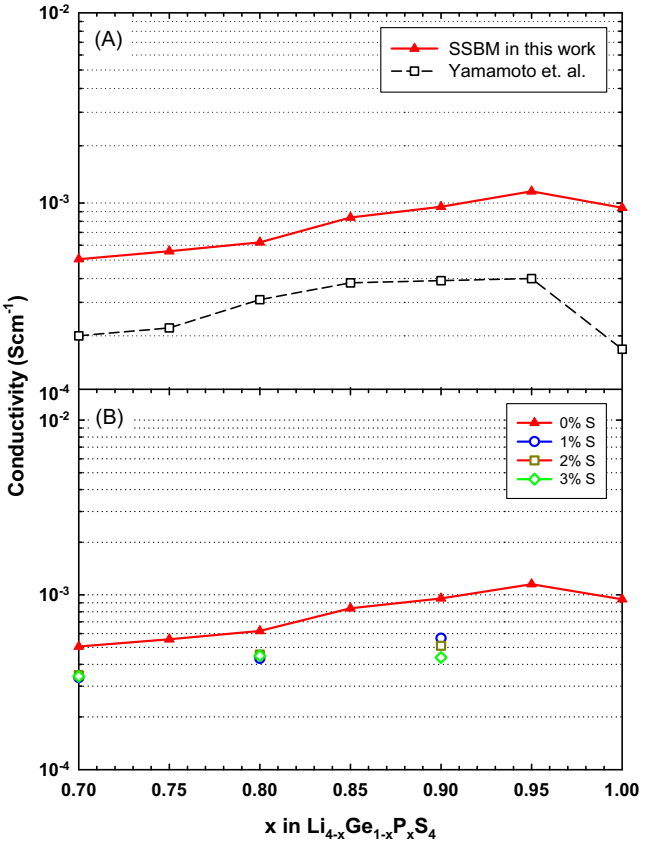

Fig. 3. (A) Conductivity of ball milled $Li_{4-x}Ge_{1-x}P_xS_4$ in this work and solid electrolyte produced by Yamamoto et al. [14]. (B) Conductivity of ball milled $Li_{4-x}Ge_{1-x}P_xS_4$ with different amount of elemental S.

involves the mixing of two kinds of network-forming sulfides P_2S_5 and GeS_2, and the presence of a large concentration of Li in the glass–ceramic materials [15]. The mixed-anion effect typically results in a higher ionic conductivity due to the introduction of more polarizable anions that can deform to stabilize transition state geometries of the migrating ion through covalent interactions between anions [14]. The high ionic conductivities may also be due to the larger ionic radii of Ge atoms which improve the mobility of the conducting species [16]. As we received our highest conductivity from the composition $x = 0.95$, we began our study using this material but found that the composition $x = 0.70$ ($71.7Li_2S$–$13.0GeS_2$–$15.2P_2S_5$) performed better for our Li/$LiCoO_2$ cells in terms of cycling stability as well as initial coulombic efficiency. Therefore, we used the material with $x = 0.70$ exclusively for heat treatment studies with adding elemental sulfur. Other compositions were initially considered and tested but did not yield significantly comparable results to that of $x = 0.70$ when heat-treated with adding elemental sulfur, which proved to be optimal for our Li/$LiCoO_2$ cells.

Table 1
Conductivity of $Li_{4-x}Ge_{1-x}P_{2(1+x)}S_{2(1-x)}$.

x	Conductivity/S cm^{-1}
0.70	5.1×10^{-4}
0.75	5.6×10^{-4}
0.80	6.2×10^{-4}
0.85	8.4×10^{-4}
0.90	9.5×10^{-4}
0.95	1.2×10^{-3}
1.00	9.4×10^{-4}

Table 2
Conductivity of $Li_{4-x}Ge_{1-x}P_xS_4$ with added sulfur.

x	S (%)	Conductivity/S cm^{-1}
70	1	3.4×10^{-4}
70	2	4.3×10^{-4}
70	3	5.6×10^{-4}
80	1	3.5×10^{-4}
80	2	4.6×10^{-4}
80	3	5.1×10^{-4}
90	1	3.4×10^{-4}
90	2	4.5×10^{-4}
90	3	4.4×10^{-4}

Ball milled powders were heat treated with numerous weight concentrations of elemental sulfur, the most significant of which are specified in Table 2 with corresponding recorded conductivities. Data were taken for 1, 2, and 3 wt.% to observe the effects of sulfur composition on conductivity. Fig. 3(B) shows a conductivity map for samples heat treated with elemental sulfur where the conductivity remains high in spite of increasing amounts of sulfur. A decreased conductivity is more pronounced with increased sulfur for samples correlating to $x = 0.90$ in $Li_{4-x}Ge_{1-x}P_xS_4$. An overall trend of decreasing conductivity can be observed for increased amounts of added sulfur, as we expected.

Fig. 4 shows the XRD patterns of the SSBM glass–ceramic electrolytes for the compositional range of $Li_{4-x}Ge_{1-x}P_xS_4$ powders for $0.70 < x < 1.00$ without HT. The gradual negative shift of the "thio-LISICON III analog" peaks (circle) starting from $x = 0.95$ and ending at $x = 0.75$ is noticeable. This could be explained by larger ionic size of Ge [16], which can enlarge the whole Li_2S–P_2S_5 lattice. One of the reasons for the increased conductivity by adding small amount

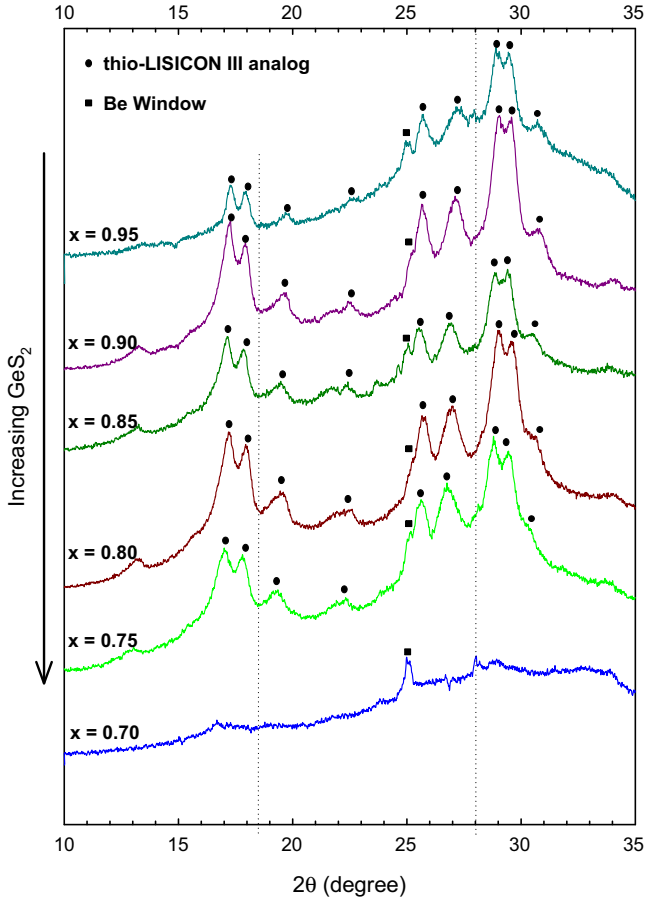

Fig. 4. XRD patterns of SSBM $Li_{4-x}Ge_{1-x}P_xS4$.

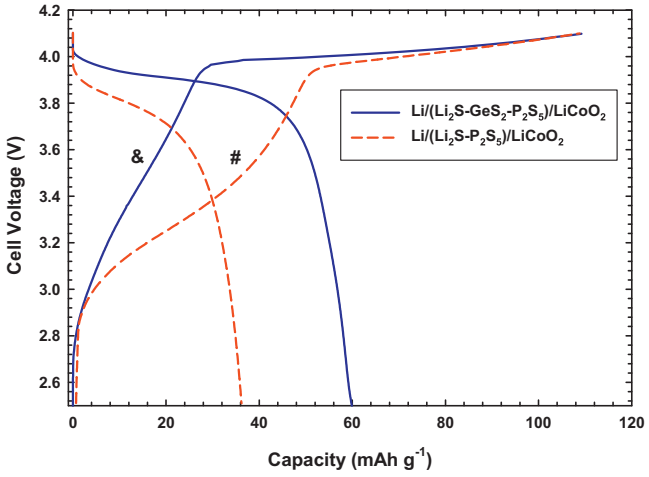

Fig. 5. First cycle voltage profiles for (a) $Li/(Li_2S–P_2S_5)/LiCoO_2$, (b) $Li/(Li_2S–P_2S_5/Li_2S–GeS_2–P_2S_5)/LiCoO_2$ double layer pellet, and (c) $Li/(Li_2S–P_2S_5/Li_2S–GeS_2–P_2S_5)/LiCoO_2$ double layer pellet with 1 wt.% elemental sulfur heat treated into the $Li_2S–GeS_2–P_2S_5$ solid electrolyte.

of GeS_2 ($x = 0.95$) in $0.75Li_2S$-$0.25P_2S_5$ ($x = 1.00$) may be explained by more open structure for better Li^+ transport by the inclusion of GeS_2. The most interesting point, however, is the close correlation that can be drawn between the changing crystal structures and the variations in electrochemical performance. The composition with the lowest conductivity among the tested compositions corresponded to the only amorphous phase of material which also represents the sample with a large overall change in the dominant crystal structure as well as the best stability and performance, especially with the inclusion of elemental sulfur. These results closely correlate to our previous findings using $GeSe_2$ as a second network former [9].

Fig. 5 shows the typical charge–discharge voltage profiles of $LiCoO_2$/Li cells using $Li_2S–GeS_2–P_2S_5$ and $Li_2S–P_2S_5$ solid-state electrolytes. The columbic efficiency for the first cycle of the samples is poor, which we attribute to the severe side reaction observed by the sloping plateau ('#') for Li_2S-P_2S_5 and ("&") for $Li_2S–GeS_2–P_2S_5$ between 2.8 and 3.9 V. The $LiCoO_2$ should ideally create a charge/discharge reaction voltage plateau at ~3.9 V. We observe that for the electrolyte containing GeS_2, the first cycle side reaction is far less severe than that of the $Li_2S–P_2S_5$ electrolyte. The inclusion of GeS_2 reduced the fraction of side reaction constituting the first cycle charge capacity from 48% for the $Li_2S–P_2S_5$ electrolyte down to 26% for the $Li_2S–GeS_2–P_2S_5$ electrolyte. A side reaction at the interface between $Li_2S–P_2S_5$ SSE and active material may be creating a larger resistance barrier than that for $Li_2S–GeS_2–P_2S_5$. When the sulfide and oxide ion-conducting species are in contact, there is a transfer of Li^+ ions forms a space-charge layer in both materials that in turn leads to interfacial resistance [9,17]. We speculate that the inclusion of GeS_2 prevents excessive side reaction by stabilizing the large chemical potential difference between the sulfur based electrolyte and the oxide based active material. While the inclusion of GeS_2 results in approximately a 50% reduction of side reaction when compared to the $Li_2S–P_2S_5$ system, further exploration is needed to resolve the large fraction of side reaction that remains. Current efforts for reduction of the side reaction revolve around improved mixing procedures for composite cathodes and utilization of size-reduced electrolyte materials. No significant side reactions were observed for subsequent cycling. However, some degradation was observed for both cells which we attribute to the increasing interfacial resistance.

Fig. 6(A) depicts capacity of $Li/LiCoO_2$ cells as a function of cycle number depending on the SSE configuration – single layer or bilayer. Previously we have shown that SSBM $77.5Li_2S–22.5P_2S_5$ is stable in contact with Li metal [13]. However, the $77.5Li_2S–22.5P_2S_5$ is not stable in contact with $LiCoO_2$ as seen in the fast capacity fading (circle) after several cycles, which drove exploration of second network formers for stabilization. Utilization of the GeS_2-based electrolyte ($Li_2S–GeS_2–P_2S_5$, $x = 0.70$ in $Li_{4-x}Ge_{1-x}P_xS_4$ with adding 1 wt.% sulfur) leads to the improvement of the capacity and cycle performance. However, it still shows capacity fading, which we found to be due to the instability of $Li_2S–GeS_2–P_2S_5$ in contact with Li metal. Consequently we constructed a bilayer electrolyte with cell configuration, $Li/(Li_2S–P_2S_5/Li_2S–GeS_2–P_2S_5)/LiCoO_2$. Fig. 6(A) shows that the bilayer SSE construction (triangle) is superior to the single layer SE ones (circle and diamond), which is attributed to the stable interfaces of both $Li/Li_2S–P_2S_5$ and $Li_2S–GeS_2–P_2S_5/LiCoO_2$.

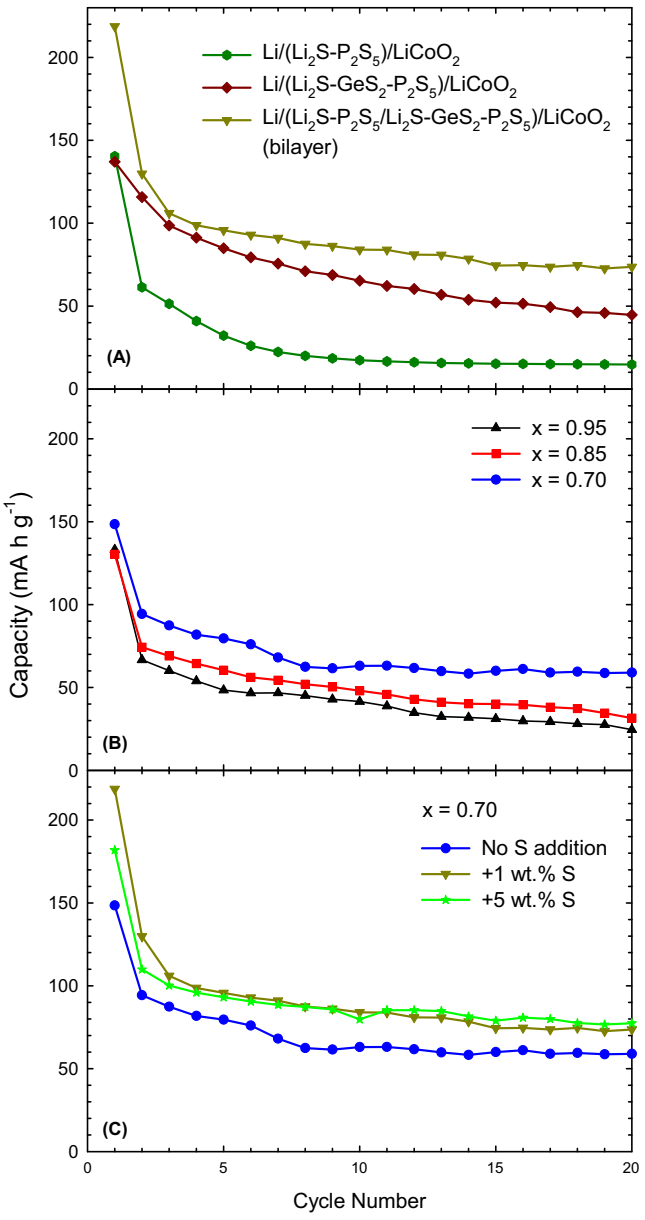

Fig. 6. (A) Charge capacity of Li/LiCoO2 as a function of cycle number depending on configuration of the SE layers (single layer or bilayer) of $0.775Li_2S–0.225P_2S_5$ and/or $Li_2S–GeS_2–P_2S_5$ ($x = 0.70$ in $Li_{4-x}Ge_{1-x}P_xS_4$ with 1 wt.% sulfur addition). (B) Effects of the amount of GeS_2 and (C) addition of sulfur on $Li_2S–GeS_2–P_2S_5$ on the cycle performance of $Li/LiCoO_2$ cell using bilayer SE consisting of SSBM $0.775Li_2S–0.225P_2S_5$ and $Li_2S–GeS_2–P_2S_5$ ($Li_{4-x}Ge_{1-x}P_xS_4$) electrolytes.

Table 3
First cycle efficiency (charge/discharge) of $Li_{4-x}Ge_{1-x}P_{2(1+x)}S_4$ based systems.

Sample (x)	Efficiency
0.70	0.63
0.75	0.57
0.80	0.56
0.85	0.55
0.90	0.52
0.95	0.49
1.00	0.42
0.70 + 1% S	0.70
0.70 + 2% S	0.65
0.70 + 3% S	0.63
0.70 + 5% S	0.60

The cycling performance of $Li/LiCoO_2$ cells using SSBM bilayer electrolytes using bilayer electrolytes, $77.5Li_2S–22.5P_2S_5/Li_2S–GeS_2–P_2S_5$ ($Li_{4-x}Ge_{1-x}P_xS_4$) with three different amounts of GeS_2 in $Li_{4-x}Ge_{1-x}P_xS_4$, agrees well with the observation that addition of GeS_2 in $Li_2S–P_2S_5$ system enhances the stability of $LiCoO_2$/SSE interface (Fig. 6(B)). Increasing the amounts of GeS_2 leads to increase the capacity and improve the cycle retention. Cells cycled at the smallest concentration of GeS_2 ($x = 0.95$) demonstrated a charge capacity of 66 mA h g^{-1} for the second cycle and the fastest rate of capacity fade in the following cycles, with only 36% retention after 20 cycles. The highest concentration of GeS_2 ($x = 0.70$), resulted in the highest second cycle charge capacity of 94 mAh g^{-1}, and the highest capacity retention of 64% after 20 cycles. The first cycle coulombic efficiency, which we define as the charge capacity divided by the discharge capacity, increased for larger amounts of GeS_2, going from approximately 49% for $x = 0.95$ up to 62% for $x = 0.70$ shown in Table 3.

Finally, in Fig. 6(C), we show that incorporation of elemental sulfur at various compositions can have significant effects on the cycling stability and first cycle coulombic efficiency. The cell with 1 wt.% added sulfur (triangle) shows the best performance with a second cycle capacity of 129 mA h g^{-1}, a 20th cycle capacity of 75 mA h g^{-1} and a first cycle coulombic efficiency of 70%. When we increased the amount of added sulfur past 1 wt.% (star), we began to see a decline in first cycle coulombic efficiency down to 60% for 5 wt.% added sulfur (Table 3), and no improvement in cycling behavior. When more than 5% wt. sulfur was added, cycling capacity degraded quite rapidly.

4. Conclusion

Glass–ceramic $Li_2S–GeS_2–P_2S_5$ ($Li_{4-x}Ge_{1-x}P_xS_4$) electrolytes with various compositions from $x = 0.70$ to $x = 1.00$ were prepared by a simple SSBM process. The $Li_2S–GeS_2–P_2S_5$ SE showed high conductivities of maximum 1.2×10^{-3} S cm^{-1} for $x = 0.95$ in $Li_{4-x}Ge_{1-x}P_xS_4$. Structural analysis showed that inclusion of GeS_2 leads to the enlarged lattice structure followed by occurrence of amorphous structure. HT of the SSBM material with 1 wt.% elemental sulfur resulted in increased capacity (129 mA h g^{-1} at the second cycle), better cycling performance and electrochemical stability of all-solid-state $LiCoO_2/Li$ cells. Instability problem of the $Li_2S–GeS_2–P_2S_5$ in contact with Li was solved by using bilayer electrolyte configuration ($Li/(Li_2S–P_2S_5/Li_2S–GeS_2–P_2S_5)/LiCoO_2$). With the observation of ionic conductivities comparable to that of liquid electrolytes, we can conclude that the inferior performances of all-solid-state cells lie with interfacial reactions and chemical instabilities.

Acknowledgments

This work has been supported by DARPA/DSO. Dr. Yoon Seok Jung acknowledges the Korea Research Foundation Grant funded by the Korean Government [KRF-2008-357-D00066].

References

[1] F. Mizuno, S. Hama, A. Hayashi, K. Tadanaga, T. Minami, M. Tatsumisago, Chem. Lett. (2002) 1244.
[2] N. Machida, H. Maeda, H. Peng, T. Shigematsu, J. Electrochem. Soc. 149 (2002) A688.
[3] A. Sakuda, H. Kitaura, A. Hayashi, K. Tadanaga, M. Tatsumisago, J. Electrochem. Soc. 156 (2009) A27.
[4] Y. Seino, K. Takada, B.C. Kim, L. Zhang, N. Ohta, H. Wada, M. Osada, T. Sasaki, Solid State Ionics 176 (2005) 2389.
[5] K. Takada, N. Ohta, L. Zhang, K. Fukuda, I.I. Sakaguchi, R. Ma, M. Osada, T. Sasaki, Solid State Ionics 179 (2008) 1333.
[6] Y. Hashimoto, N. Machida, T. Shigematsu, Solid State Ionics 175 (2004) 177.
[7] K. Takada, T. Inada, A. Kajiyama, M. Kouguchi, H. Sasaki, S. Kondo, Y. Michiue, S. Nakano, M. Tabuchi, M. Watanabe, Solid State Ionics 172 (2004) 25.
[8] A. Hayashi, S. Hama, H. Morimoto, M. Tatsumisago, T. Minami, J. Am. Ceram. Soc. 84 (2001) 477.
[9] J.E. Trevey, Y.S. Jung, S.H. Lee, J. Power Sources 195 (2010) 4984.
[10] M. Tatsumisago, Solid State Ionics 175 (2004) 13.
[11] M. Tatsumisago, F. Mizuno, A. Hayashi, J. Power Sources 159 (2006) 193.
[12] F. Mizuno, A. Hayashi, K. Tadanaga, M. Tatsumisago, Adv. Mater. 17 (2005) 918.
[13] J.E. Trevey, J.S. Jang, Y.S. Jung, C.R. Stoldt, S.H. Lee, Electrochem. Commun. 11 (2009) 1830.
[14] A.R. West, Solid State Chemistry and it's Applications, Wiley, 1984.
[15] H. Yamamoto, N. Machida, T. Shigematsu, Solid State Ionics 175 (2004) 707.
[16] R. Kanno, M. Murayama, J. Electrochem. Soc. 148 (2001) A742.
[17] N. Ohta, K. Takada, L. Zhang, R. Ma, M. Osada, T. Sasaki, Adv. Mater. 18 (2006) 2226.